JOURNAL OF MATERIALS SCIENCE 27 (1992) 2267–2271

The dielectric properties of zirconia

D. P. THOMPSON, A. M. DICKINS
Wolfson Laboratory, Materials Division, Department of Mechanical, Materials and Manufacturing Engineering, University of Newcastle upon Tyne, Newcastle upon Tyne NE17RU, UK

J. S. THORP
School of Engineering and Applied Science, University of Durham, Durham, UK

The dielectric properties of a series of single-crystal and sintered polycrystalline zirconias have been measured at room temperature over the frequency range 1–12.5 kHz. The additive cations investigated were yttrium, magnesium, calcium and cerium. For monoclinic zirconia, it was found that the permittivity, ε', was 23 at 10 kHz, in agreement with previous work. The addition of stabilizing cations causes a substantial increase in ε' which then lies in the range 32–42 depending on the nature and amount of the stabilizing cation. Analysis of the separate contributions to the overall permittivity arising from the monoclinic, tetragonal or cubic phases has been made for some mixed-phase systems. The results suggest that the permittivity is principally determined by the crystallographic form rather than by the nature or amount of the added cation.

1. Introduction

Very few measurements of dielectric properties of zirconia and its solid solutions have been reported in the literature, and among these there is a considerable spread in values for nominally similar materials. Thus different sources give the permittivity for the same material varying by up to a factor of two; for example, for calcium-stabilized zirconia ε' has been reported as being 16 or 26, and for monoclinic zirconia values are quoted from 13.5–24 [1, 2]. This is in part due to the measurement techniques used: for example, estimating permittivity from the refractive index of thin films makes assumptions about the magnetic properties of the material, whilst experiments on powders introduce uncertainty when trying to deduce the properties of the bulk material by allowing for the porosity of the powder. Work on single crystals has been limited only to monoclinic zirconia [1], and yttria-stabilized zirconia (YSZ) [3]. The present paper reports dielectric data on a range of zirconias, using samples of sintered polycrystalline materials, and repeats the previous single-crystal YSZ measurements at audio frequencies.

Stabilized and partially stabilized zirconias are made by sintering pure zirconia with varying amounts of other oxides, which results in a solid solution with the additive cation becoming incorporated into the zirconia lattice by substitution for zirconium. Pure zirconia has a monoclinic (m-) unit cell at room temperature, but the added cations stabilize a higher symmetry tetragonal (t-) or cubic (c-) unit cell with corresponding changes in lattice parameters. An additive which is not iso-valent with zirconium will produce oxygen-defects with resulting non-stoichiometry.

2. Experimental procedure

The materials used in this study are listed in Table I, and were obtained from three sources. Most samples were in the form of nuggets of sintered polycrystals (supplied by United Ceramics, Stafford, UK). These materials were inhomogeneous in colour due to local variations in impurity levels and slight compositional departure (by reduction) from ZrO_2. Most of these samples have been labelled by the additive cation and its amount in weight per cent, whereas the sample of monoclinic zirconia was referenced Z-100. The manufacturer's stated impurity levels were $< 0.1\%$ for magnesia, alumina, iron(III) oxide and sodium oxide, and $< 0.15\%$ for silica. Sample Y-3 was prepared from Toyo Soda 3 mol % yttria TZP (tetragonal zirconia polycrystals) by cold-compacting the as-received powder, iso-statically pressing to 2500 p.s.i. (10^3 p.s.i. $= 6.89\ \mathrm{N\,mm^{-2}}$) and sintering at 1400 °C for 1 h. The remaining two samples were single-crystal fully stabilized zirconias with nominally 8 and 12 mol % yttria.

All samples were examined to determine their crystal form using a Hägg–Guinier focusing X-ray powder camera, and the results processed by a least-squares computer program to give accurate values of the lattice parameters. The amount of monoclinic phase present in each sample, expressed as a volume fraction, θ, was estimated from diffractometer traces by comparing the relative intensities of particular diffracted lines [4]. If the integrated intensity from the $(h\,k\,l)$ plane is $I(h\,k\,l)$, then

$$\theta = \frac{1.603 I(1\,1\,\bar{1})_{\mathrm{m}}}{1.603 I(1\,1\,\bar{1})_{\mathrm{m}} + I(1\,1\,1)_{\mathrm{t+c}}} \qquad (1)$$

The permittivity and dielectric loss (tan δ) were determined from measurements of capacitance and conductance using a bridge method [5]. Samples were cut on a diamond wheel to give square slices approximately 10 mm × 10 mm × 0.5 mm, and 6 mm diameter gold electrodes were evaporated on opposite

TABLE I Lattice parameters for all samples (θ = volume fraction of monoclinic phase; V = unit cell volume)

Sample	Additive	Monoclinic						Tetragonal			Cubic	
	(Nominal)	θ (%)	a (nm)	b (nm)	c (nm)	β	V (10^{-3} nm^3)	a (nm)	c (nm)	V (10^{-3} nm^3)	a (nm)	V (10^{-3} nm^3)
Z-100	None	100	0.5138	0.5203	0.5298	80°53′	139.84					
Mg-3.5	3.5 wt % MgO	45	0.5139	0.5177	0.5314	80°50′	139.57	0.508	0.529	136.52		
Ce-14	14 wt % CeO_2	44	0.5192	0.5218	0.5309	79°19′	141.34	0.5208	0.5255	142.53		
Ca-5	5 wt % CaO	5						0.5114	0.5138	134.37		
Y-3	3 mol % Y_2O_3	10						0.5102	0.5175	133.71	0.5137	135.56
Y-6	6 wt % Y_2O_3	10	0.5153	0.5107	0.5169	81°21′	134.48	0.5099	0.5171	134.44		
Y-8	8 mol % Y_2O_3	0									0.5138	135.64
Y-12	12 mol % Y_2O_3	0									0.5148	136.43

faces to ensure good electrical contact. Measurements were made using either a Wayne–Kerr bridge type B 224, operating in the frequency range 1–12.5 kHz selected using a Farnell oscillator, or a Topward RLC meter type 5100. The calculation to obtain ε′ and tan δ used corrections to allow for any stray capacitance in the leads or jig, or for effects of conduction over the surface of the specimen [6]. Samples were dried with a hot air blower before measurement to remove any surface moisture.

3. Results

3.1. Crystallographic measurements

The results of the X-ray work are summarized in Table I. Sample Z-100 has lattice parameters in close agreement (0.1%) with published values (e.g. JCPDS Powder Diffraction File, card 36-420), while the small variations in unit cell dimensions of the monoclinic phases in other samples are the result of slight accommodation of the additive cations. Direct comparisons with the literature can be made for the yttria–zirconia system (which is well documented) but not for the other systems. In Fig. 1, the lattice parameters for the yttria-containing samples (Y-3, Y-6, Y-8 and Y-12) are plotted as a function of yttria content together with values taken from the literature [7, 8]. Although the cubic cell parameters agree very well, the fit for the tetragonal phases is not as good. This is due to the difficulty in measuring the X-ray pattern of tetragonal phases, the lines of which are generally indistinct and sometimes overlap with reflections from the other zirconia polymorphs.

3.2. Dielectric measurements

The frequency variation of permittivity and dielectric loss for all samples is shown in Figs 2 and 3, respectively. For the majority of samples, both responses are nearly frequency independent over the whole range. The two exceptions are Z-100 and Ce-14 which show marked low-frequency rises in both graphs. This nonlinearity is discussed later. The permittivity measured

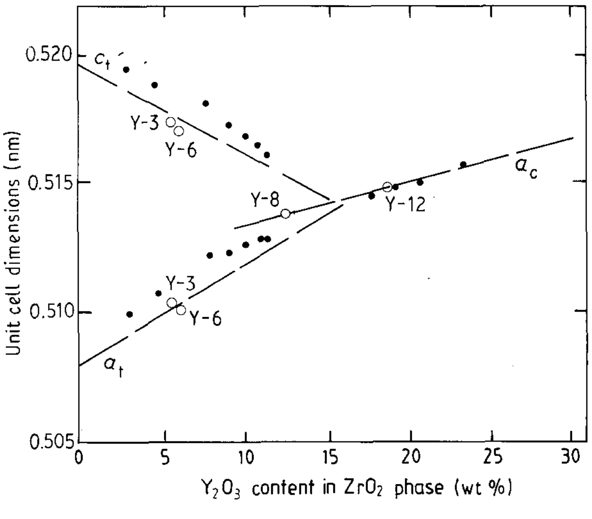

Figure 1 The effect of yttria content on cell dimensions for YSZ. (——) Scott [7], (●) Cheng and Thompson [8].

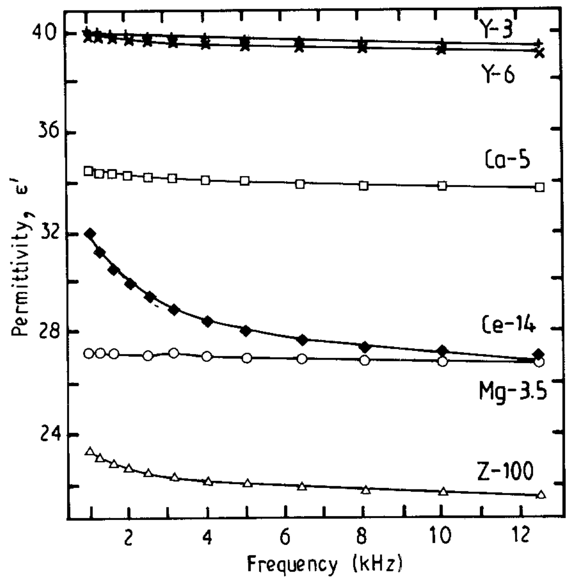

Figure 2 Permittivity, ε', as a function of frequency, *f*.

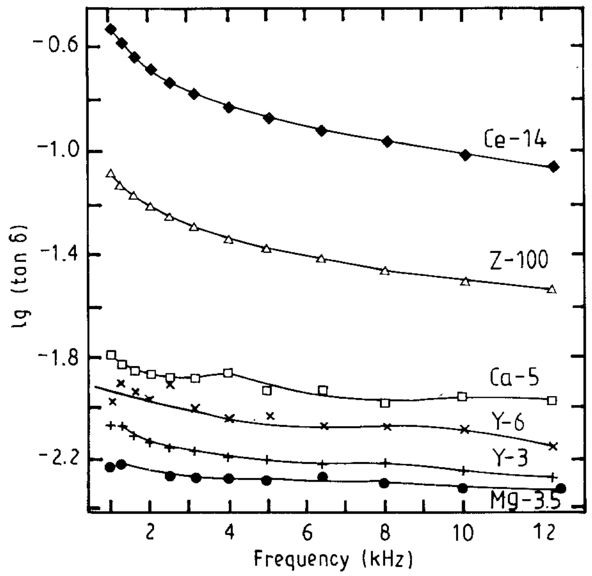

Figure 3 Dielectric loss, tan δ, as a function of frequency, *f*.

TABLE II Comparison between ε' at 10 kHz for two sets of samples

	Sample				
	Z-100	Mg-3.5	Ce-14	Ca-5	Y-6
Wayner-Kerr bridge	22.0	27.2	27.3	34.0	39.0
RLC meter	25.3	27.6	32.8	34.7	[a]

[a] Poor quality sample.

on a second set of the samples showed close agreement with the first, and comparative results at 10 kHz are given in Table II. No loss data were available because the conductance of the specimens was below the detection threshold of the meter. A selection of literature data for zirconia materials is shown in Table III. Samples 1, 2 and 7 are in good agreement with the present results, whilst the low values for Samples 3 and 6 are no doubt due to inadequate correction for the porosity in the powder samples used. The level of additive in Samples 4 and 5 was not stated but must be high because the crystals were fully stabilized.

4. Discussion

We consider first the frequency-variation of ε'. The flatness of the responses in Figs 2 and 3 suggests that the "universal law" applies [9–11], so that

$$(\varepsilon' - \varepsilon_\infty) \propto \omega^{(n_1 - 1)} \tag{2}$$

$$\varepsilon'' \propto \omega^{(n_2 - 1)} \tag{3}$$

where ω is the angular frequency, and ε_∞ the limit of ε' at high frequency. Table IV shows values of the exponent n obtained from log–log plots of ε' and ε'' against frequency. It is noticeable that n_1 (the value derived from ε') is close to unity, whereas n_1 and n_2 are not, in general, equal. Previous studies on magnesium oxide [5] and on some oxynitride glasses [12] have shown that in pure materials limited by lattice loss, n_1 and n_2 have identical values very close to unity. In less pure materials, however, e.g. in black alumina [13] and in black aluminium nitride [14], a similar disparity between n_1 and n_2 has been observed. For any one material measured in the present study, n_1 and n_2 are not particularly close, especially for the Z-100 and Ce-14 samples. This behaviour is due to space-charge polarization in these two samples [15] which results in the measured permittivity being higher than its true value at low frequencies. This has been confirmed by measurements using a Q-meter, which show that the permittivity at 10 kHz is almost the same at 1 and 10 MHz.

Secondly, it is interesting to note the effect of the amount of stabilizing cation on ε' in the yttria–zirconia system (see Fig. 4). The addition of a small amount of yttria nearly doubles the permittivity of zirconia (from ε' = 23 for Z-100 to ε' = 40 for Y-3), while still higher levels of the dopant cause transformation to c-symmetry and a gradual decrease in ε'. This can be substantially explained by the discontinuous drop in unit cell volume of about 5% with the m → t transformation, whereas the volume change for t → c is

TABLE III Some literature values of ε' for zirconias

Sample	Material	ε'	Frequency	Comments	Reference
1	Monoclinic	22 ± 1	0.1–20 kHz	Single crystal	[1]
2	Monoclinic	24 ± 1	1 MHz	Liquid immersion method	[1]
3	Monoclinic	13.5	"Audio"	Powder	[2]
4	MgO-stabilized	27 ± 1	Not stated	Fully cubic polycrystals	[1]
5	CaO-stabilized	26 ± 4	Not stated	Fully cubic polycrystals	[1]
6	CaO-stabilized	16–17	"Audio"	10 mol %, powder	[1]
7	Y_2O_3-stabilized	38 ± 4	Audio	8 wt % single crystal	[3]

TABLE IV Values of the exponent n

Sample	n_1 (from ε')	n_2 (from ε'')
Z-100	0.98	0.56
Ce-14	0.95	0.47
Mg-3.5	0.99	0.84
Ca-5	0.97	0.87
Y-6	0.99	0.80
Y-3	0.99	0.91

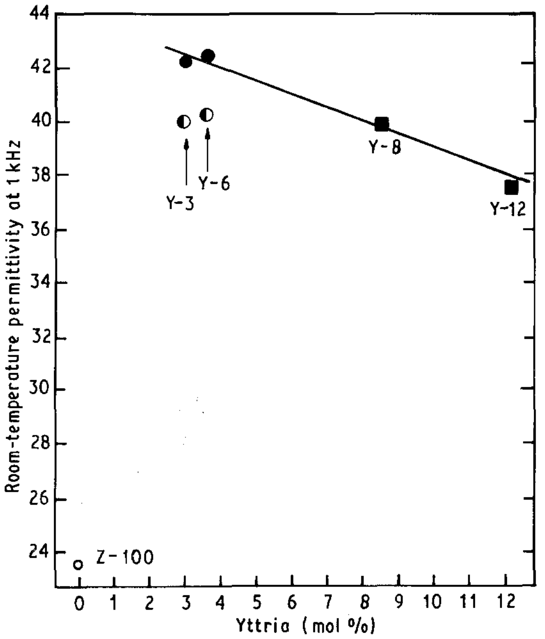

Figure 4 The effect of yttria content on the permittivity of YSZ. Phases: (○) monoclinic, m; (●) tetragonal, t; (◐) mixed m and t; (■) cubic, c.

a small and continuous increase. The dependence of ε' on unit cell volume is described by the Clausius–Mosotti equation

$$\frac{\varepsilon' - 1}{\varepsilon' + 2} = \frac{\alpha}{3V\varepsilon_0} \tag{4}$$

where ε' is the permittivity of the bulk material, α is the polarizability of a unit cell with volume V, and ε_0 is the permittivity of free space. At the m → t transformation, there is a large increase in ε', due to a sudden decrease in unit cell volume. A smaller contribution to ε' results from changes in the polarizability of the unit cell and also because of the more ionic nature of the t- and c-phases compared with m. The observed changes in ε' (23–40) correspond to a change of about 5% in the LHS of Equation 4, which is consistent with the change in unit cell volume.

For the t- and c-phase, there is a gradual decrease in ε' with increasing amounts of additive, with a continuous change at the t → c transformation. This is again because the unit cell polarizability changes only slowly with the accommodation of more of the additive cations, while V increases more significantly (see Table I and Fig. 1). It is the reduction in the number of polarizable particles per unit volume which results in a decrease in ε'.

This result, that ε' is principally determined by the crystallographic form rather than by the nature and amount of additive, is supported by the data for the other samples. However, it has been necessary to characterize the samples more precisely for two reasons. Firstly, the solubility of additives in the m-phase is negligibly small so that, when both m- and t-phases are present, the concentration of additive in the phase is higher than that for the sample as a whole. Table V lists for each two-phase sample the amounts of additive in the t-phase, calculated by assuming that there is none at all in the m-phase. Secondly, for those samples which are two-phase mixtures, Lichtenecker's mixing rule [16–18] gives

$$\log \varepsilon' = \theta \log \varepsilon'_m + (1 - \theta) \log \varepsilon'_t \tag{5}$$

where ε'_m is the permittivity of the m-phase, ε'_t is that for the t-phase, and ε' is the measured permittivity of the sample. The volume fraction of m-phase, θ, has been determined for all samples. Because the solubility of additive cations in the m-phase is small, ε'_m may be assumed to remain constant, being 23 at 10 kHz as determined for Z-100. Hence the permittivity of the t-phases may be derived from measurements on the mixed-phase samples by re-arranging Equation 5 to give

$$\varepsilon'_t = \left(\frac{\varepsilon'}{\varepsilon'^{\theta}_m}\right)^{1/(1-\theta)} \tag{6}$$

From the values in Table V, it is seen that ε'_t is in the range 32–42, depending on the nature of the stabilizing cation. Some spread is to be expected from the differences in ionic polarizability of the various cations, while the values of ε'_t for the yttria-containing samples are close.

A similar dependence of permittivity on the amount of additive cation has been found for calcia-stabilized zirconia [2]. In this case, ε' was reported to increase from 13.5 for monoclinic zirconia to a maximum of 17–19 corresponding to 12 mol% CaO, with higher concentrations of additive causing a decrease in ε'. These permittivities are noticeably lower than those in the present paper, but the low values are undoubtedly due to using powdered samples, in which the volume fraction of air was greater than one-half. An analysis of the contributions to permittivity from the different crystal phases is not possible as the necessary crystallographic information was not given.

With regard to the dielectric loss (Fig. 3), samples stabilized with magnesium, calcium or yttrium show $\tan \delta$ to be in the range $1\text{–}2 \times 10^{-3}$ with little dependence on frequency. The losses of Z-100 and Ce-14 are

TABLE V Calculated permittivities, ε'_t, for the tetragonal zirconias, at 10 kHz

Sample	ε'	θ (%)	ε'_t	Cation in t-phase (wt %)
Mg-3.5	27.2	45	32.4	6.4
Ca-5	34.0	< 5	34.5	5.3
Ce-14	27.3	44	32.3	24.3
Y-3	39.5	10	42.0	6.0
Y-6	39.0	10	41.6	6.7

both considerably higher, with a low-frequency rise similar to that observed with the permittivity for these two samples. It is noticeable that Fig. 3 suggests that for all the materials the loss converges to a value of about 10^{-3} at high frequency. On the basis of the present data, it is not possible to deduce any systematic variation of loss with, for example, type and amount of additive cations, porosity, or the concentration of anion vacancies. Contrary to the results for the permittivity, crystal structure appears to play very little part in determining the observed loss.

5. Conclusions

For monoclinic zirconia, $\varepsilon' = 23$ at 10 kHz. When a stabilizing cation (yttrium, magnesium, calcium or cerium) is used to stabilize a higher symmetry crystal phase, i.e. tetragonal or cubic, the permittivity changes in a way which can be quantitatively explained by the Clausius–Mosotti equaton. The dielectric loss (tan δ) of these materials is generally about 0.01.

Acknowledgements

This work was carried out with the support of the Procurement Executive, Ministry of Defence. The authors are grateful for helpful discussions with Dr B. Mortimer and Mr P. Tattershall, Royal Aerospace Establishment, Farnborough, and one of us (A.M.D.) also appreciates the award of a post-graduate scholarship.

References

1. P. J. HARROP and J. N. WANKLYN, *Brit. J. Appl. Phys.* **18** (1967) 739.
2. M. SANESI and G. CREMANTE, *Z. Naturforsch.* **26A** (1971) 159.
3. J. S. THORP and H. P. BUCKLEY, *J. Mater. Sci.* **8** (1973) 1401.
4. D. L. PORTER and A. H. HEUER, *J. Amer. Ceram. Soc.* **62** (1979) 298.
5. J. S. THORP and N. ENAYATI-RAD, *J. Mater. Sci.* **16** (1981) 255.
6. A. H. SCOTT and H. L. CURTIS, *J. Res. Nat. Bur. Stand.* **22** (1939) 747.
7. H. G. SCOTT, *J. Mater. Sci.* **10** (1975) 1527.
8. Y. CHENG and D. P. THOMPSON, *Brit. Ceram. Trans. J.* **87** (1988) 107.
9. A. K. JONSCHER, *Nature* **253** (1975) 717.
10. *Idem, ibid.* **250** (1970) 191.
11. *Idem, ibid.* **267** (1977) 673.
12. S. V. J. KENMUIR, J. S. THORP and B. L. J. KULESZA, *J. Mater. Sci.* **18** (1983) 1725.
13. J. S. THORP, M. AKHTARUZZAMAN and D. EVANS, *ibid.* **25** (1990) 4143.
14. J. S. THORP, D. EVANS, M. AL-NAIEF and M. AKHTARUZZAMAN, *ibid.* **25** (1990) 4965.
15. K. V. RAO and A. SMAKULA, *J. Appl. Phys.* **36** (1965) 2031.
16. K. LICHTENECKER, *Phys. Z.* **27** (1926) 115.
17. *Idem, ibid.* **32** (1931) 255.
18. A. BÜCHNER, *Wiss. Veröff. Siemens* **18** (1939) 204.

Received 18 June
and accepted 23 July 1991